DTU

ISNET-9 May 22-24 2023

Washington University in St. Louis

Information and Statistics for Nuclear Experiments and Theory workshop

Workshop 24 crow 201/Compton 241/245

Symposium in Honor of John Clark

Physicist at the computational Frontier (H.Bohr)

John W. Clark

Wayman Crow Professor Emeritus of Physics

PHD, WASHINGTON UNIVERSITY IN ST. LOUIS
M.A. PHYSICS, UNIVERSITY OF TEXAS, AUSTIN
B.S. PHYSICS, UNIVERSITY OF TEXAS, AUSTIN

DEPARTMENT OF PHYSICS ↗

PUBLICATIONS LIST ↗

MCDONNELL CENTER FOR THE SPACE SCIENCES ↗

research interests:

Quantum Many-Particle Theory • Dense-Matter Astrophysics • Neural Networks • Quantum Control

DTU

John W Clark

FOLLOW

Wayman Crow Professor of Physics, Washington University
Verified email at physics.wustl.edu - Homepage
Quantum many-body theory   nuclear theory   strongly correlated electron…   neural networks

TITLE	CITED BY	YEAR
On the controllability of quantum-mechanical systems GM Huang, TJ Tarn, JW Clark Journal of Mathematical Physics 24 (11), 2608-2618	490	1983
Detecting network communities by propagating labels under constraints MJ Barber, JW Clark Physical Review E 80 (2), 026129	435	2009
Variational theory of nuclear matter JW Clark Progress in particle and nuclear physics 2, 89-199	359	1979
Method of correlated basis functions JW Clark, P Westhaus Physical Review 141 (3), 833	205	1966
Pairing gaps in nucleonic superfluids JMC Chen, JW Clark, RD Davé, VV Khodel Nuclear Physics A 555 (1), 59-89	187	1993
Proton superfluidity in neutron-star matter NC Chao, JW Clark, CH Yang Nuclear Physics A 179 (2), 320-332	140	1972
Solution of the gap equation in neutron matter VA Khodel, VV Khodel, JW Clark Nuclear Physics A 598 (3), 390-417	138	1996
Simplified treatment for strong short-range repulsions in n-particle systems. i. general theory JW Clark, E Feenberg Physical Review 113 (2), 388	128	1959
Cluster Expansions in Many-Fermion Theory. I.``Factor-Cluster"Formalisms JW Clark, P Westhaus	126	1968
Topology of the Fermi surface beyond the quantum critical point VA Khodel, JW Clark, MV Zverev Physical Review B 78 (7), 075120	118	2008
Nucleonic superfluidity in neutron stars: 1S0 neutron pairing in the inner crust JMC Chen, JW Clark, E Krotscheck, RA Smith Nuclear Physics A 451 (3), 509-540	118	1986
Tensor correlations in nuclear matter ML Ristig, WJ Ter Louw, JW Clark Physical Review C 3 (4), 1504	118	1971
Superfluidity in nuclear systems and neutron stars A Sedrakian, JW Clark The European Physical Journal A 55, 1-56	115	2019
Progress in particle and nuclear physics JW Clark Pergamon, Oxford	115	1979
Superfluid condensation energy of neutron matter CH Yang, JW Clark Nuclear Physics A 174 (1), 49-62	107	1971
Anomalous low-temperature behavior of strongly correlated Fermi systems JW Clark, VA Khodel, MV Zverev Physical Review B 71 (1), 012401	101	2005
Nuclear mass systematics using neural networks S Athanassopoulos, E Mavrommatis, KA Gernoth, JW Clark Nuclear Physics A 743 (4), 222-235	98	2004
Studies in the method of correlated basis functions:(II). Graphical analysis and integral equation methods E Krotscheck, JW Clark Nuclear Physics A 328 (1-2), 73-103	98	1979
Neural network modelling JW Clark Physics in Medicine & Biology 36 (10), 1259	96	1991
Chaos in neural systems KE Kürten, JW Clark Physics Letters A 114 (7), 413-418	93	1986

John W. Clark, Whyman-Crow professor. Emeritus of physics, Washington University

- John Clark. A great internationally renown scientist with a large production of famous articles in a large range of research fields.
- He has been a great teacher of scientific deciplines and lead many PhD-students to a succesful carrier.
- He has been pionered or started new fields of research within the area of theoretical physics and applied phycics such as neural nets
- His wide range of professionalism and excellency have amaized all scientists and students.
- ”Du hast perlen und diamanten mein lieber, -was willst du doch meer” (Heine).

On the controllability of quantum-mechanical systems

Garng M. Huang and T. J. Tarn
Department of Systems Science and Mathematics, Washington University, St. Louis, Missouri 63130
John W. Clark
Department of Physics and McDonnell Center for the Space Sciences, Washington University, St. Louis, Missouri 63130

(Received 25 August 1981; accepted for publication 10 June 1983)

The systems-theoretic concept of controllability is elaborated for quantum-mechanical systems, sufficient conditions being sought under which the state vector ψ can be guided in time to a chosen point in the Hilbert space $\mathscr{H}$ of the system. The Schrödinger equation for a quantum object influenced by adjustable external fields provides a state-evolution equation which is linear in ψ and linear in the external controls (thus a bilinear control system). For such systems the existence of a dense analytic domain $\mathscr{D}_\omega$ in the sense of Nelson, together with the assumption that the Lie algebra associated with the system dynamics gives rise to a tangent space of constant finite dimension, permits the adaptation of the geometric approach developed for finite-dimensional bilinear and nonlinear control systems. Conditions are derived for global controllability on the intersection of $\mathscr{D}_\omega$ with a suitably defined finite-dimensional submanifold of the unit sphere $S_{\mathscr{H}}$ in $\mathscr{H}$. Several soluble examples are presented to illuminate the general theoretical results.

PACS numbers: 03.65.Bz, 02.20.Sv

Superfluidity in nuclear systems and neutron stars

Armen Sedrakian[1] and John W. Clark[2,3]

[1] Frankfurt Institute for Advanced Studies, Ruth-Moufang str. 1, D-60438 Frankfurt am Main, Germany
[2] Department of Physics and McDonnell Center for the Space Sciences, Washington University, St. Louis, MO 63130, USA
[3] Centro de Investigação em Matemática e Aplicações, University of Madeira, 9020-105 Funchal, Madeira, Portugal

Received: 23 June 2019 / Revised: 8 August 2019 / Published online: 30 September 2019

Communicated by N. Alamanos

Abstract. Nuclear matter and finite nuclei exhibit the property of superfluidity by forming Cooper pairs. We review the microscopic theories and methods that are being employed to understand the basic properties of superfluid nuclear systems, with emphasis on the spatially extended matter encountered in neutron stars, supernova envelopes, and nuclear collisions. Our survey of quantum many-body methods includes techniques that employ Green functions, correlated basis functions, and Monte Carlo sampling of quantum states. With respect to empirical realizations of nucleonic and hadronic superfluids, this review is focused on progress that has been made toward quantitative understanding of their properties at the level of microscopic theories of pairing, with emphasis on the condensates that exist under conditions prevailing in neutron-star interiors. These include singlet S-wave pairing of neutrons in the inner crust, and, in the quantum fluid interior, singlet-S proton pairing and triplet coupled P-F-wave neutron pairing. Additionally, calculations of weak-interaction rates in neutron-star superfluids within the Green function formalism are examined in detail. We close with a discussion of quantum vortex states in nuclear systems and their dynamics in neutron-star superfluid interiors.

PACS. 97.60.Jd Neutron stars – 21.65.+f Nuclear matter – 47.37.+q Hydrodynamic aspects of superfluidity; quantum fluids – 67.85.+d Ultracold gases, trapped gases – 74.25.Dw Superconductivity phase diagrams

Nuclear Physics A540 (1992) 1–26
North-Holland

NUCLEAR PHYSICS A

Learning and prediction of nuclear stability by neural networks

S. Gazula and J.W. Clark

McDonnell Center for the Space Sciences and Department of Physics, Washington University, St. Louis, MO 63130, USA

H. Bohr

School of Chemical Sciences, University of Illinois, Urbana, IL 61801, USA

Received 17 June 1991
(Revised 21 November 1991)

Abstract: The backpropagation learning algorithm is used to teach layered feedforward networks of model neurons the existing data on nuclear stability and atomic masses. Specific applications include (i) the construction of networks that decide stability, (ii) learning and prediction of nuclear mass excesses and (iii) analysis of the systematics of neutron separation energies. With suitable architecture and representation of input and output data, learning can be accomplished with high accuracy. Evidence is presented that these new adaptive computational systems can grasp essential regularities of nuclear physics including the valley of β-stability, the pairing effect and the existence of shell structure. Significant predictive ability is demonstrated, opening the prospect that neural networks may provide a valuable new tool for computing nuclear properties and, more broadly, for phenomenological description of complex many-body systems.

Citations per year

Nuclear shell model for the elements

Relative Abundance for different even-even nuclides as fct of A.

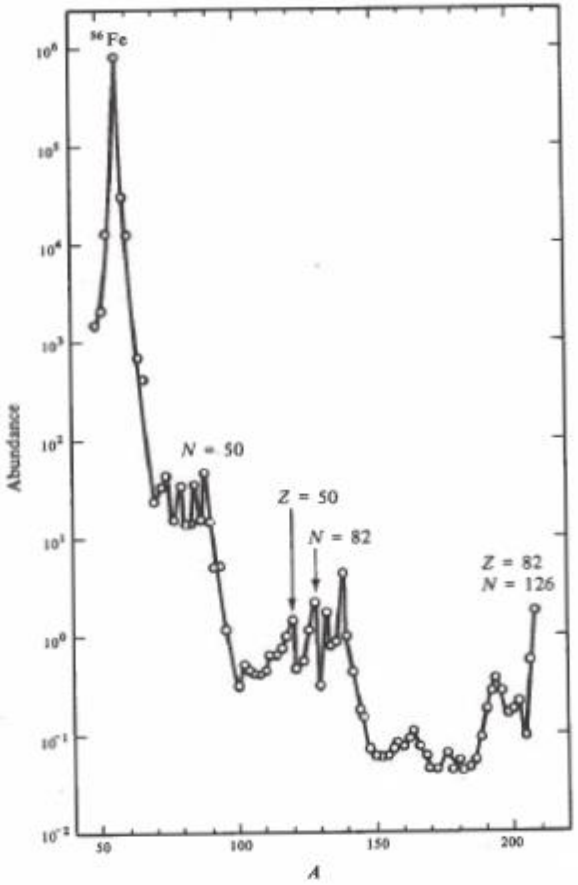

Fig. 15.1. Relative abundance, *H*, for different even-even nuclides, plotted as a function of *A*. The abundances are measured relative to Si, with *H*(Si) = 10^6. [Based on A.G.W. Cameron, "A New Table of Abundance of the Elements in the Solar System," *Origin and Distribution of the Elements* (L. H. Arens, ed.), Pergamon Press, New York, 1968, p. 125.]

responsible for the pronounced peaks: If the last electron fills a major shell, it is particularly tightly bound, and the separation energy reaches a peak. The next electron finds itself outside a closed shell, has very little to hold onto, and can be removed easily. The nuclear quantity that is analogous to the ionization potential is the separation energy of the last nucleon. If, for

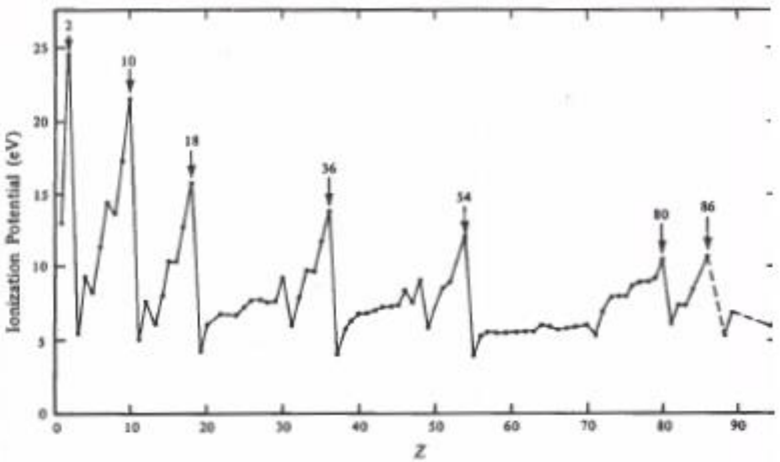

Fig. 15.2. Separation energies of the neutral atoms (ionization potentials). (Based on data from C. E. Moore, "Ionization Potentials and Ionization Limits Derived from the Analyses of Optical Spectra," *NSRDS—NBS 34*, 1970.)

instance, a neutron is removed from a nuclide (Z, N), a nuclide $(Z, N-1)$ results. The energy needed for removal is the difference in binding energies between these two nuclides,

$$S_n(Z, N) = B(Z, N) - B(Z, N-1). \qquad (15.2)$$

An analogous expression holds for the proton separation energy. With Eqs. (14.3) and (14.4), the separation energy can be written in terms of the mass excesses,

$$S_n(Z, N) = m_n c^2 - u + \Delta(Z, N-1) - \Delta(Z, N) \qquad (15.3)$$

or with the numerical values of the neutron mass and the atomic mass unit

$$S_n(Z, N) = 8.07 \text{ MeV} + \Delta(Z, N-1) - \Delta(Z, N).$$

The mass excess is given in Table A6 in the Appendix, and the separation energy can be computed quickly. The result can be presented in two different ways: either Z can be kept fixed, or the neutron excess $N - Z$ can be kept constant. The first situation is easier to visualize: We start with a certain nuclide, continue adding neutrons, and record the energy with which each one is bound. Such a plot is shown in Fig. 15.3 for the isotopes of cerium, $Z = 58$. Two effects are apparent, an even-odd difference and a closed-shell discontinuity. The even-odd behavior indicates that neutrons are more tightly bound when N is even than when N is odd. The same holds for protons. This fact, together with the empirical observation that all even-even nuclei have spin zero in their ground states, shows that an extra attractive interaction occurs when two like particles pair off to zero angular

Input and output simplicity

Nuclear structure contains two important input:

- number of protons
- number of neutrons,

Which could give rise to a lot of outputs:

- Mass
- Separation energy
- Spin
- Charge
- Strange particles from strange quarks

The simple input of the neural networks prediction for the isotopes is in contrast to patient diagnosis, where the number of inputs are hundredfold

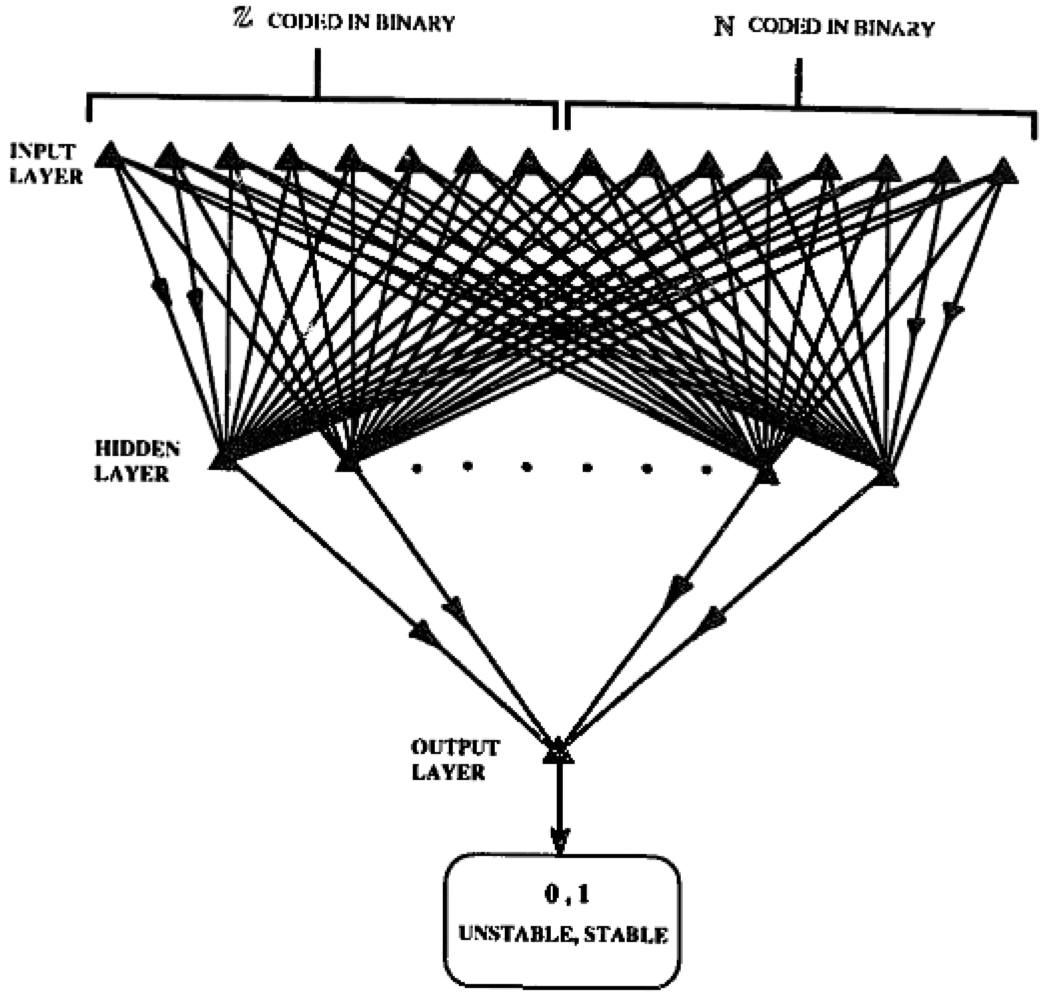

Fig. 1. Feedforward neural network that is taught to distinguish between stable and unstable nuclides. Target outputs are indicated in the window at the bottom. The network type is ${}^{b}(16 + H + 1)_{a}$.

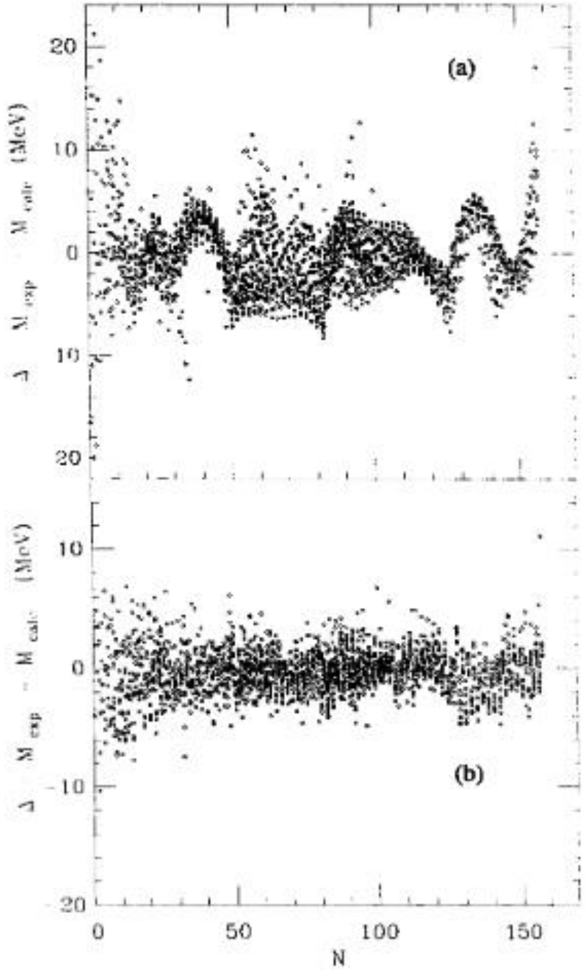

Fig. 3. Deviations $\Delta(Z,N) = M_{exp} - M_{calc}$ of learned values of atomic masses from their experimental values, projected on a plane perpendicular to the Z-axis. (a) Results for a $^{a}(2+20+1)_{a}$ net with analog input coding and analog output coding. (b) Results for a $^{b}(16+20+1)_{a}$ net with binary input coding and analog output coding. For reference, the range of database masses is given approximately by $M_{exp} = [-92, 128]$ MeV.

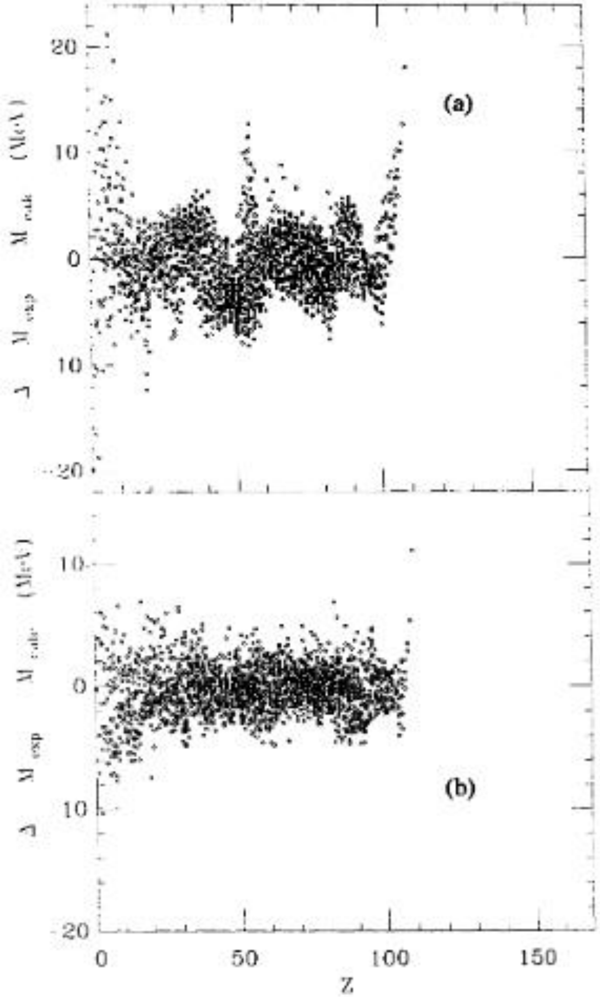

Fig. 4. Same as fig. 3, except that the error surface is projected on a plane perpendicular to the *N*-axis.

$$\sigma_{\mathrm{r.m.s.}} = \left[\sum_{\mu} (M_{\mathrm{exp}}^{(\mu)} - M_{\mathrm{calc}}^{(\mu)})^2/n\right]^{1/2} \tag{5}$$

and the mean deviation

$$\overline{D} = \sum_{\mu} (M_{\mathrm{calc}}^{(\mu)} - M_{\mathrm{exp}}^{(\mu)})/n\,. \tag{6}$$

The sums include the n patterns in the training or test set, as appropriate. For learning, $\sigma_{\mathrm{r.m.s.}}$ is directly proportional to the square root of the cost function (assuming single-unit analog output coding). The mean error $\overline{D}$ characterizes the systematic overbinding or underbinding by the model in fitting or prediction.

The performance of neural-network mass models in the predictive mode is of paramount interest, since this approach might offer a valuable new tool for interpolation between known nuclides, and possibly for modest extrapolation on the fringes of the existing data base. In table 1 we have collected the results of representative learning runs on the reduced data base, and of subsequent predictive runs for the remaining test nuclides. All training sessions were long enough that the learning process had effectively reached completion. Nevertheless, substantial fluctuations in the cost

TABLE 1

Errors in learning and prediction of atomic masses by feedforward neural networks of various types. The measures $\sigma_{r.m.s.}$ and $\overline{D}$ are respectively the root-mean-square and mean errors defined by eqs. (5) and (6), respectively. Learning refers to the reduced data base of 1719 nuclei, prediction to the reserved test sample of 572. The last two lines give the error measures for two of the best traditional mass models[21,27,22]), which use respectively 1504 and 1593 database nuclei and 471 and 26 adjustable parameters. Units are MeV.

Net type	Learning error		Prediction error	
$^c(I + H_1 + \cdots + H_L + O)_{c'}[P]$	$\sigma_{r.m.s.}$	$\overline{D}$	$\sigma_{r.m.s.}$	$\overline{D}$
$^a(2 + 20 + 1)_a[81]$	5.254	1.165	5.100	1.001
$^a(2 + 60 + 1)_a[241]$	4.342	1.054	4.340	0.885
$^a(2 + 90 + 1)_a[361]$	10.219	5.086	10.231	5.041
$^a(2 + 10 + 10 + 1)_a[151]$	2.796	−1.192	2.929	-1.242
$^b(16 + 20 + 1)_a[361]$	2.013	1.156	2.278	−0.038
$^b(16 + 10 + 10 + 1)_a[291]$	1.499	−0.362	2.180	−0.278
$^b(16 + 10 + 10 + 10 + 1)_a[401]$	1.156	0.308	3.612	0.396
$^b(16 + 10 + 10 + 14 + 1)_a[449]$	1.569	−0.669	2.180	−0.559
Masson–Jänecke fit [471]	0.346	0.014	–	–
Möller–Nix fit [26]	0.849	0.013	–	–

TABLE 2

Root-mean-square and mean errors, $\sigma_{r.m.s.}$ and $\overline{D}$, made by feedforward neural networks after training on the full data base of 2291 atomic masses. Units are MeV.

Net type	Learning error	
[c] $(I + H_1 + \cdots + H_L + O)_{c'}[P]$	$\sigma_{r.m.s.}$	$\overline{D}$
[a] $(2 + 20 + 1)_a[81]$	3.384	0.313
[a] $(2 + 60 + 1)_a[241]$	3.848	0.362
[a] $(2 + 10 + 10 + 1)_a[151]$	1.807	−0.053
[b] $(16 + 20 + 1)_a[361]$	1.919	0.268
[b] $(16 + 10 + 10 + 10 + 1)_a[401]$	1.008	0.005
[b] $(16 + 10 + 10 + 14 + 1)_a[449]$	0.932	−0.049
[b] $(18 + 10 + 10 + 10 + 1)_a[421]$	0.697	0.010

- Neural network prediction for separation energy for:

  N-Z=19,

- where the prediction is given by the dotted line (indicated through the red arrows)
- Predicted through an (18+18+18) network

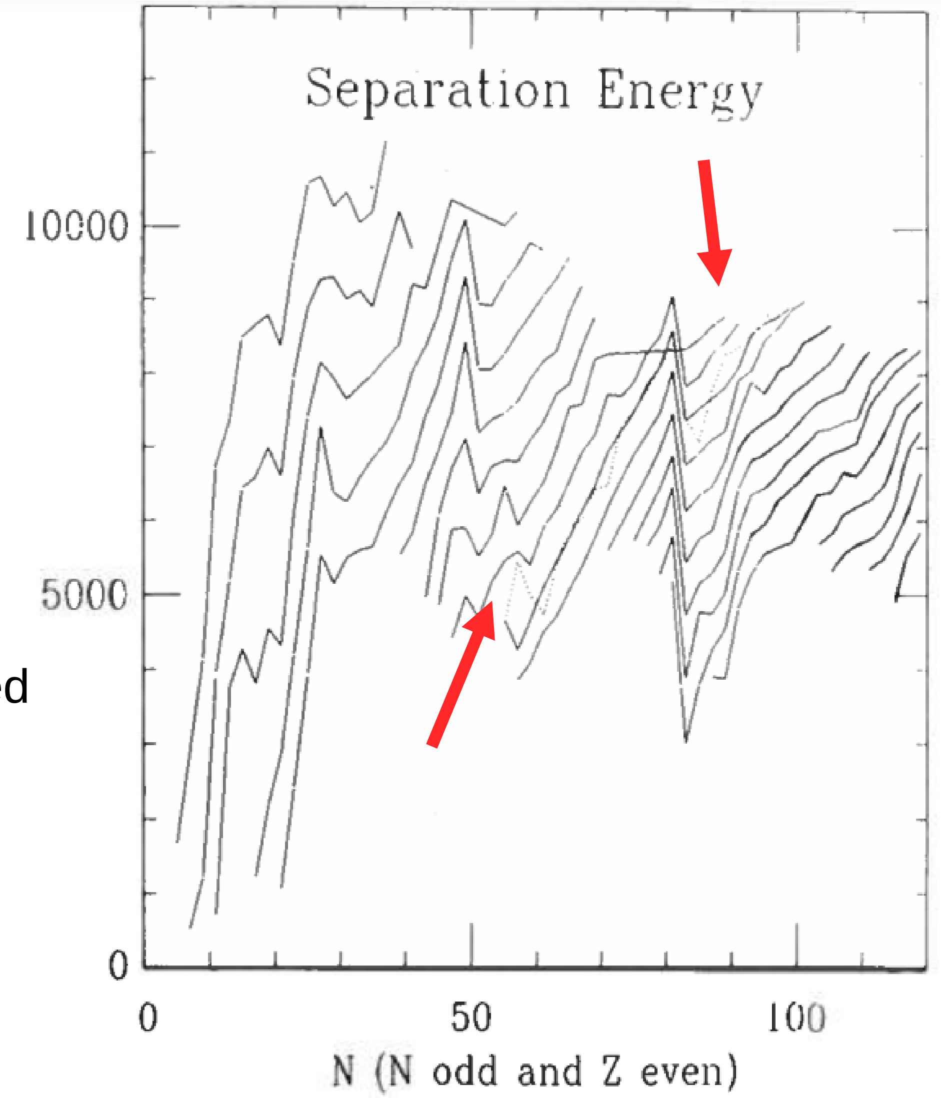

Fig. 5. Data points for neutron separation energies (in keV) of odd-N–even-Z nuclei of given $N - Z$ are connected by solid lines. Dotted curve shows prediction of $N - Z = 19$ line by a (18 + 18 + 18), network with semi-optimized real-number coding schemes for input and output variables.

TABLE 3

Errors in learning and prediction of neutron separation energies for odd-N, even-Z nuclei by neural networks with real-number input and output coding. The quoted learning ("learn") errors refer to the accuracy of response on the 90% of the database used in training, and the prediction ("pred") errors, to that on the remaining 10%. Values of $\sigma'_{r.m.s.}$ are in MeV.

Net type	$\sigma'_{r.m.s.}$ (learn)	$\overline{d}'$ (learn)	$\sigma'_{r.m.s.}$ (pred)	$\overline{d}'$ (pred)
$^{r}(10+10+9)_{r}[209]$	0.143	1.63%	0.160	1.8%
$^{r}(18+18+18)_{r}[684]$	0.098	0.89%	0.117	1.6%
$^{r}(18+38+18)_{r}[1424]$	0.095	0.69%	0.197	1.9%